Adsorption Kinetics, Isotherms, and Thermodynamics of Removal of Anionic Surfactant from Aqueous Solution Using Fly Ash

by Arif Hidayat

Adsorption Kinetics, Isotherms, and Thermodynamics of Removal of Anionic Surfactant from Aqueous Solution Using Fly Ash

Ahmer Ali Siyal · **Rashid Shamsuddin** ·
Aaron Low · **Arif Hidayat**

Abstract Surfactants are organic compounds which can be used in several applications. However, they can contaminate world water resources causing detrimental effects to human beings, aquatic life, and animals. This paper investigates the adsorption kinetics, isotherms, and thermodynamic properties for the removal of an anionic surfactant, sodium dodecylbenzene sulfonate (SDBS), using fly ash. Characteristics of fly ash such as surface area and pore size analysis and the point of zero charge (PZC) were determined. The effects of parameters such as pH, surfactant concentration, and temperature and the adsorption kinetics, isotherms, and thermodynamic properties and adsorption mechanism were determined. Fly ash is a mesoporous material having surface area and pore size of 1.079 m^2/g and 9.813 nm and PZC at pH 6.58. pH 2 and the temperature 25 °C were optimum for adsorbing SDBS onto fly ash. The adsorption capacity and removal efficiency increased by increasing the concentration of SDBS from 100 to 2000 mg/L, indicating that the increase of surfactant concentration could not saturate the surface of fly ash. The pseudo-second-order and the Langmuir isotherm models showed best fit to the adsorption data and the thermodynamic properties described adsorption as an exothermic, barrierless, non-spontaneous, and entropy-reducing reaction which is more feasible at a lower temperature of 25 °C. This indicated that the adsorption occurs by both physisorption and chemisorption with monolayer coverage of SDBS on the surface of fly ash. SDBS surfactant adsorbed onto fly ash mainly through electrostatic interactions between oppositely charged SDBS and fly ash.

Keywords Surfactant · Wastewater · Adsorption · Isotherm · Kinetics · Thermodynamic properties

A. A. Siyal · R. Shamsuddin (✉)
HICoE, Centre for Biofuel and Biochemical Research (CBBR), Institute for Sustainable Living, Department of Chemical Engineering, Universiti Teknologi PETRONAS, 32610 Bandar Seri Iskandar, Perak Darul Ridzuan, Malaysia
e-mail: mrashids@utp.edu.my

A. Low
Ligar LP, 10 Bisley Road, Ruakura Research Campus, Hamilton, New Zealand

A. Hidayat
Department of Chemical Engineering, Universitas Islam Indonesia, Jalan Kaliurang km.14.5, Ngemplak, Sleman D.I., Yogyakarta 55584, Indonesia

1 Introduction

The world's water resources are contaminated by the release of many pollutants into water sources such as rivers, streams, and oceans. Surfactants are the emerging water pollutants regularly observed in wastewater. They are hazardous compounds which can have negative effects on the environment (eutrophication) as well as on humans, animals, and fish (cancer, endocrine disruption, dermatitis, eye irritation, and pathological, physiological, and biological effects) (Kimerle and Swisher 1977; Önder et al. 2007; Pal et al. 2013; Pereira et al. 2015). The increased use of surfactants and disposal of

untreated wastewater containing surfactants into water resources represent an environmental threat to the world.

Surfactants are chemical compounds which possess both hydrophobic and hydrophilic components. They are categorized into three classes such as ionic (anionic and cationic), nonionic, and amphoteric on the basis of charge on the head group. They are used in detergents, emulsion stabilization, foaming, wetting, pharmaceutical formulations, mineral separations, and many other purposes (Bautista-Toledo et al. 2014). Worldwide, 12 MT of surfactants is used per year in domestic and industrial applications (Edser 2008; Beltrán-Heredia et al. 2012). The consumption of anionic surfactants is large worldwide as they are simple and economical to manufacture while providing good foaming and washing properties (Zanoletti et al. 2017). The surfactant concentration ranges from 1 to 10 mg/L in domestic wastewater and approximately 300 mg/L from surfactant manufacturing industries wastewater (Zhang et al. 1999).

Methods such as coagulation (Aboulhassan et al. 2006), chemical and electrochemical oxidation (Ikehata and El-Din 2004; Panizza et al. 2005), microbial treatment (Pérez-Carrera et al. 2010; Tezel et al. 2012), ion exchange, adsorption (Gonzalez-Garcia et al. 2002; Schouten et al. 2007; Sineva et al. 2007), foam separation (Boonyasuwat et al. 2003), and membrane separation (Kowalska 2011) can be used to remove surfactants from wastewater. The use of most of these methods is limited by the effectiveness, economic feasibility, and environmental friendliness. Adsorption is the most commonly used method for surfactant removal due to its effectiveness, cost, and environmental friendliness. A variety of adsorbents such as multi-walled carbon nanotubes (MWCNTs) (Ncibi et al. 2015), silica nanoparticles functionalized with amine groups (Kim, Kim et al. 2019), polymer resin (Gönder et al. 2010), fly ash/TiO$_2$ composite (Visa and Duta 2013), amino cross-linked chitosan microspheres (ACCMs) (Zhang et al. 2017), and pine tree cone activated carbon (Valizadeh et al. 2016) have been introduced for anionic surfactant removal from wastewater. Fly ash showed 96% removal of an anionic surfactant, sodium dodecylsulfate (SDS), and an adsorption capacity of 0.96 mg/g was achieved at a fly ash dose of 100 g/L (Zanoletti et al. 2017).

Adsorption kinetics describes rates of reactions and phenomena of adsorption. The pseudo-first-order, pseudo-second-order, and intraparticle diffusion models are

commonly used to model the adsorption kinetics of surfactants. The pseudo-first-order model described the kinetics of removing the anionic surfactant sodium dodecylbenzene sulfonate (SDBS) using pine tree cone activated carbon and commercial activated carbon (Bautista-Toledo et al. 2014). The intraparticle diffusion and pseudo-second-order models described the kinetics of SDBS, cetyltrimethylammonium bromide (CTAB), and Triton X-100 (TX-100) surfactants onto MWCNTs (Ncibi et al. 2015).

Adsorption isotherms are used to determine the equilibrium of an adsorption reaction (Siyal et al. 2020; Zulfiqar et al. 2020). The Langmuir, Freundlich, and Temkin models are commonly used to model the adsorption of surfactants. The Langmuir model described the removal of anionic and cationic surfactants such as sodium lauryl ether sulfate (SLES) and CTAB using polymer resin VPOC 1064 MD PH and indicated the process as a monolayer (Gönder et al. 2010). The Freundlich model described the removal of the nonionic eicosaneoxyethylene hexadecyl ether (POE type) surfactants and the anionic SDS using Pittsburgh activated carbon in both single and multi-solute modes and indicated the adsorption as multilayer (Asakawa and Ogino 1986). Thermodynamic properties such as activation energy (E_a), Gibbs free energy ($\Delta G°$), enthalpy ($\Delta H°$), and entropy ($\Delta S°$) are determined to understand the nature of adsorption. The changes in the Gibbs free energy of removal of n-dodecyl-β-$_D$-maltoside (DM) and sucrose capric acid (SMD) (disaccharide-based surfactants) and sucrose lauric acid (SML) described that the decrease of temperature from 313 to 293 K decreased the surfactants' tendency of adsorption and the adsorption tendency of mono- and disaccharide sugar surfactants depended on the structure of the polar part of surfactants while temperature did not affect adsorption (Krawczyk 2018). However, the adsorption kinetics, isotherms, and thermodynamic properties of adsorption of the anionic surfactant SDBS onto the fly ash have never been studied.

This paper reports adsorption kinetics, isotherms, and thermodynamic properties of removal of the anionic surfactant SDBS using the fly ash adsorbent. Initially, the characteristics of fly ash such as surface area, pore size, pore volume, and point of zero charge (PZC) are investigated. After the characterization of the coal fly ash, the effects of adsorption parameters such as pH, initial SDBS concentration, and temperature are investigated. Finally, the adsorption data was modeled using

kinetics and isotherm models and thermodynamic property equations. The adsorption mechanism is also described.

2 Materials and Methods

Materials Fly ash obtained from a local thermal power station was used in this study; its chemical composition is shown in Table 1. More characteristics of the fly ash such as functional groups analysis, microstructural analysis, and phase analysis are reported elsewhere (Siyal et al. 2016). Analytical reagent (AR) grade sodium dodecylbenzene sulfonate (SDBS, $C_{18}H_{29}NaO_3S$) surfactant, nitric acid (HNO_3), and sodium hydroxide (NaOH) were purchased from Sigma Aldrich, Malaysia.

2.1 Methods

2.1.1 Characterization of Fly Ash

Surface Area and Pore Size Analysis of Fly Ash The surface area, average pore size, and total pore volume of fly ash were determined using a Micromerics ASAP 2020 BET instrument through N_2 gas adsorption-desorption isotherms. The Brunauer-Emmett-Teller (BET) equation was used for determining the surface area.

Point of Zero Charge of Fly Ash Three different weight percent (wt.%) concentrations of fly ash (10, 20, and 30) were prepared in deionized water. The PZC was determined through titration. A pH meter (Eutech Instruments) was used for recording the charge density of the solutions. 0.01 M HNO_3 and 0.01 M NaOH solutions were used for adjusting the charge on the fly ash adsorbent.

2.1.2 Adsorption of SDBS onto Fly Ash

The adsorption of SDBS was conducted on a model wastewater prepared in the laboratory. SDBS model solutions ranging from 50 to 1000 mg/L were prepared by diluting 1000 mg/L SDBS stock solution with distilled water. The surfactant solution pH was adjusted to the required pH using 0.01 M NaOH and 0.01 M HNO_3. A total of 200 mL of the model wastewater solution was treated with 10 g/L of adsorbent in a conical flask. The

solutions were agitated at 200 rpm and room temperature 25 °C for 300 min (5 h) using an orbital shaker (SSM1, mini orbital shaker, Stuart, UK). Samples were taken and filtered (syringe filters 0.22 μm, Thermo Scientific) at time intervals of 0, 5, 15, 30, 60, 120, 180, 240, and 300 min. The supernatant was analyzed using a Shimadzu UV-1800 spectrophotometer set at a wavelength of 223 nm. A calibration curve prepared using SDBS concentrations in the range of 5 to 100 mg/L was used to calculate the SDBS concentration in the treated solutions. The absorbance of SDBS solutions above 100 mg/L was determined by diluting the samples up to calibration curve range before analysis on the spectrophotometer. The adsorption capacity and removal efficiency of fly ash adsorbent for SDBS surfactant were calculated using Eqs. (1) and (2), respectively.

$$q_t = \frac{V_s(C_i - C_f)}{m} \qquad (1)$$

$$\text{Removal Efficiency } (\%) = \frac{(C_i - C_f)}{C_i} \times 100 \qquad (2)$$

where

q_t Adsorption capacity at time t (mg/g),
V_s Solution volume (L),
C_i Initial surfactant concentration (mg/L),
C_f Final surfactant concentration (mg/L),
m Weight of adsorbent (g).

Effect of Binding Parameters The effects of pH, surfactant concentration, and temperature were determined by single parameter variation. The pH was varied from 2 to 10 (2, 4, 6, 8, and 10), SDBS concentration was varied from 100 to 2000 mg/L (100, 200, 300, 400, 500, 750, 1000, 1250, 1500, 1750, and 2000 mg/L), and temperature was varied from 25 to 65 °C (25, 35, 45, 55, and 65 °C). The parameter range was chosen from previous studies and trial runs (Gupta et al. 2003; Taffarel and Rubio 2010; Zanoletti et al. 2017).

Adsorption Kinetics Adsorption kinetics was used to determine the rate and mechanism of adsorption using kinetics models of the pseudo-first-order, pseudo-second-order, and the Weber intraparticle diffusion models. The adsorption data was fitted linearly to kinetics models using Origin software (Origin Pro 9.0,

Table 1 Oxide composition of fly ash (Siyal et al. 2016)

	Oxide									
	SiO_2	Al_2O_3	CaO	Fe_2O_3	MgO	K_2O	SO_3	Na_2O	TiO_2	Others
Composition (wt.%)	43.25	20.58	11.11	12.48	3.75	1.98	1.45	0.95	0.88	3.57

OriginLab Corporation). The kinetics models are given in Table 2.

Adsorption Isotherm Adsorption isotherms are used to determine the equilibrium of adsorption and adsorbent-adsorbate interactions (Shamsuddin et al. 2014). The adsorption data was linearly fitted to Langmuir, Freundlich, and Temkin isotherm models shown in Table 2 using Origin Pro software.

Thermodynamic Properties The distribution coefficient (K_d) is the amount of surfactant adsorbed onto the adsorbent in relation to the quantity of surfactant remaining in solution at equilibrium and it was determined using Eq. (3). The following equations were used to determine the thermodynamic properties of E_a, $\Delta H°$, and $\Delta S°$ (Eq. 4) and $\Delta G°$ (Eq. 5):

$$K_d = \frac{q_e}{C_e} \tag{3}$$

$$\log K_d = \frac{\Delta S°}{2.303\,R} - \frac{\Delta H°}{2.303\,RT} \tag{4}$$

$$\Delta G° = \Delta H° - T\Delta S° \tag{5}$$

3 Results and Discussion

3.1 Characterization of Fly Ash Adsorbent

3.1.1 Surface Area and Pore Size Analysis

The surface characteristic results of fly ash adsorbent are shown in Table 3. Surface area, average pore size, and total pore volume of fly ash adsorbent are 1.079 m^2/g, 9.813 nm, and 0.0026 cm^3/g respectively. The surface area of fly ash is very low compared with that of activated carbon (1201 m^2/g), multi-walled carbon nanotubes (233 m^2/g), and fly ash-TiO_2 composite (37.97 m^2/g) which have been used for the removal of anionic surfactants (Visa and Duta 2013; Ncibi et al. 2015; Valizadeh et al. 2016). The surface area of fly ash is 21% lower than of unexpanded perlite (1.22 m^2/g) which was used to adsorb the cationic CTAB surfactant (Alkan et al. 2005). The pore size results show that the fly ash is a mesoporous material. The microporous materials cannot capture the long-chain surfactant molecules at the typical size of < 2 μm. Macroporous and mesoporous materials are more feasible for absorbing large molecules due to their pore size which can easily capture larger sized surfactant molecules (De Gisi 2016). A summary of pore size analysis results along with its comparison to MWCNTs and pine tree cone activated carbon adsorbents used for SDBS removal is given in Table 3. Although the surface area of fly ash is low as compared with that of other adsorbents used for the removal of SDBS surfactant, the performance of fly ash for the removal of heavy metals, dyes, and anionic surfactant SDS from wastewater shows that fly ash can also be tested for the removal of the anionic surfactant SDBS (Wang et al. 2005, 2008; Zanoletti et al. 2017).

3.1.2 Point of Zero Charge Analysis of Fly Ash

The PZC of fly ash occurs at pH 6.58. This indicates that fly ash will be positively charged below pH 6.58 and negatively charged above pH 6.58. The hydrogen ion (H^+) concentration increases below pH 6.58 and hydroxide ion (OH^-) concentration increases above pH 6.58. The PZC results show that the pH in the acidic range will be more favorable for the anionic surfactant SDBS removal due to the higher affinity between the oppositely charged adsorbent and adsorbate. pH in the basic range will result in lower adsorption of the SDBS surfactant due to repulsion between the similarly charged components.

Table 2 Equilibrium and linearized kinetics and isotherm equations

Models	Equilibrium	Linearized	Ref.
Pseudo-first-order	$q_t = q_e\left(1 - e^{-k_1 t}\right)$	$\ln(q_e - q_t) = \ln q_e - k_1 t$	(Lagergren 1898)
Pseudo-second-order	$q_t = \frac{q_e^2 k_2 t}{(1 + q_e} k_2 t)$	$t/q_t = 1/k_2 q_e^2 + t/q_e$	(Ho and McKay 1999)
Intraparticle diffusion	$q_t = k_{int} t^{1/2}$	$q_t = k_{id} t^{0.5} + C$	(Weber and Morris 1963)
Langmuir	$Q_e = \frac{q_m b C_e}{1 + b C_e}$	$\frac{C_e}{q_e} = \frac{1}{q_m b} + \frac{C_e}{q_m}$	(Langmuir 1918)
Freundlich	$Q_e = K_f C_e^n$	$\log q_e = \mathrm{Log}\, K_F + \frac{1}{n} \log C_e$	(Freundlich 1907)
Temkin	$q_e = \frac{RT}{b} \ln(K_T C_e)$	$Q_e = B\, \mathrm{Ln}\, K_T + B\, \mathrm{Ln}\, Ce$	(Temkin 1941)

Where

q_t - Mass of surfactant adsorbed at time t (mg/g),

q_e - Mass of surfactant adsorbed at equilibrium (mg/g),

k_1 - Pseudo-first-order rate constant (1/min),

k_2 - Pseudo-second-order rate constant (g/mg min),

$k_2 q_e^2$ - Initial sorption rate also represented by h,

C - Intercept,

k_{id} - Intraparticle diffusion rate constant (mg/g day$^{0.5}$),

C_e - Equilibrium concentration of surfactant (mg/L),

q_m - Maximum adsorption at monolayer coverage (mg/g),

b - Adsorption equilibrium constant related to energy of adsorption (L/mg),

K_F - Freundlich parameter [(mg g^{-1}) * (L/mg)$^{(1-n/n)}$],

n - Freundlich parameter related to surface heterogeneity,

B - RT/b_T,

b_T - Temkin isotherm constant (J/mol),

K_T - Model constant (L/g),

B - Constant related to heat of sorption,

R - Gas constant ($R = 8.314$ J/mol. K),

T - Temperature (K).

Table 3 Characteristics of FA and other adsorbents for SDBS removal

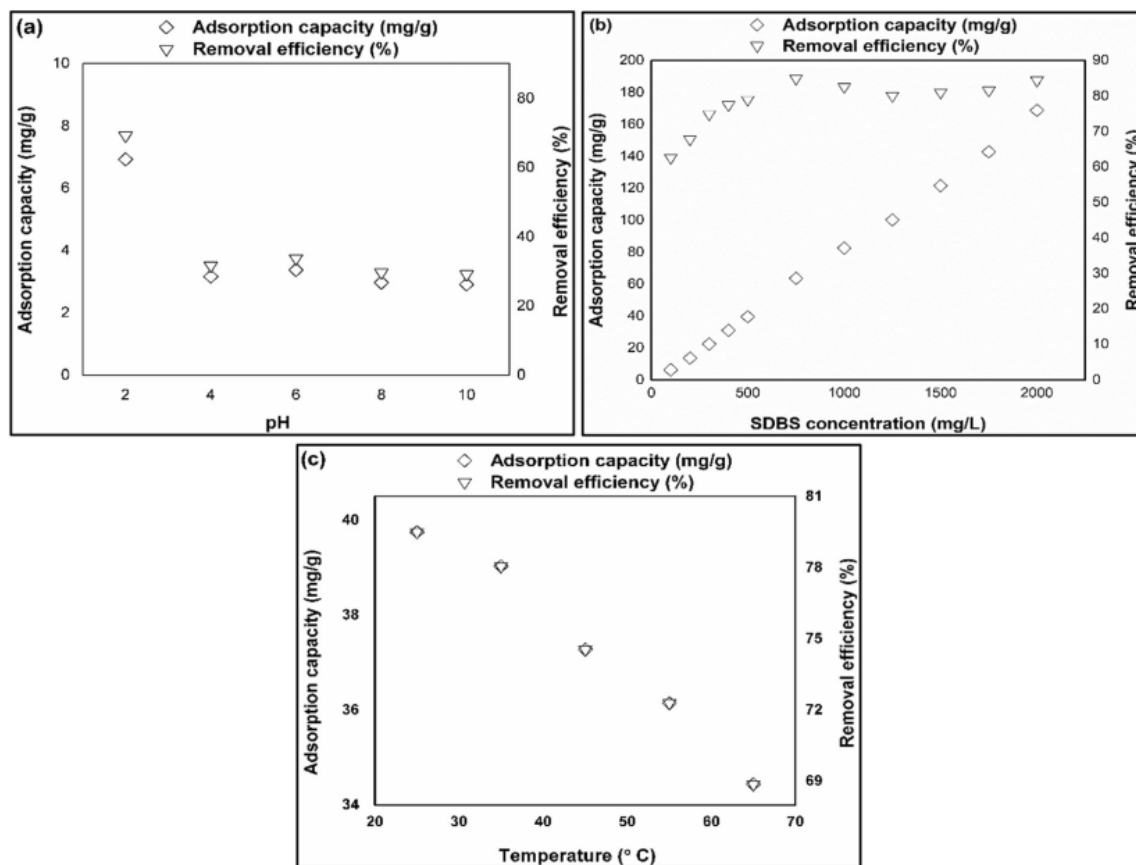| Adsorbent	Characteristics			Reference
	Surface area (m^2/g)	Pore size (nm)	Pore volume (cm^3/g)	
Fly ash	1.079	9.813	0.0026	(Siyal et al. 2019)
Multi-walled carbon nanotubes (MWCNTs)	233	1–49	0.423	(Ncibi et al. 2015)
Activated carbon from cones of pine trees	1201	2.58	0.775	(Valizadeh et al. 2016)

Fig. 1 Effect of **a** pH, **b** SDBS concentration, and **c** temperature on adsorption of SDBS

3.2 Adsorption of SDBS Surfactant Using Fly Ash Adsorbent

The effects of pH, SDBS concentration, and temperature on the adsorption of SDBS onto fly ash were investigated. Initially, an SDBS concentration of 100 mg/L was used for determining the effect of other parameters. A total of 10 g/L of fly ash and a contact time of 300 min (5 h) were chosen to be used in this study based on information from a previous study (Siyal et al. 2018).

3.2.1 Effect of pH

The effect of varying pH on the removal of SDBS using the fly ash is shown in Fig. 1a. The increase of the pH from 2 to 10 reduced the adsorption capacity from 6.922 to 2.916 mg/g and the removal efficiency from 69.22 to 29.17%. This is most likely due to the change in the affinity of fly ash for SDBS. The pH 2 gave highest adsorption capacity and removal efficiency. Fly ash is positively charged at pH 2 (pH < PZC); this could help it adsorb a higher quantity of negatively charged SDBS surfactant due to attraction between the oppositely charged adsorbent and adsorbate. The hydrogen ion (H^+) concentration increases at pH 2 which react with sulfonate groups (SO_3^-) of SDBS causing higher adsorption of SDBS surfactant onto the fly ash. Increasing the pH from 2 to 10 shifts the charge on the fly ash from positively charged to negatively charged, therefore increasing the repulsion between fly ash and SDBS. This results in decreasing adsorption capacity and removal efficiency. The data confirmed that pH 2 is optimum for the SDBS adsorption onto fly ash. pH 2 as optimum was consistent with previous research on SDBS removal using cross-linked chitosan films and the geopolymer (Kahya et al. 2018; Siyal et al. 2019).
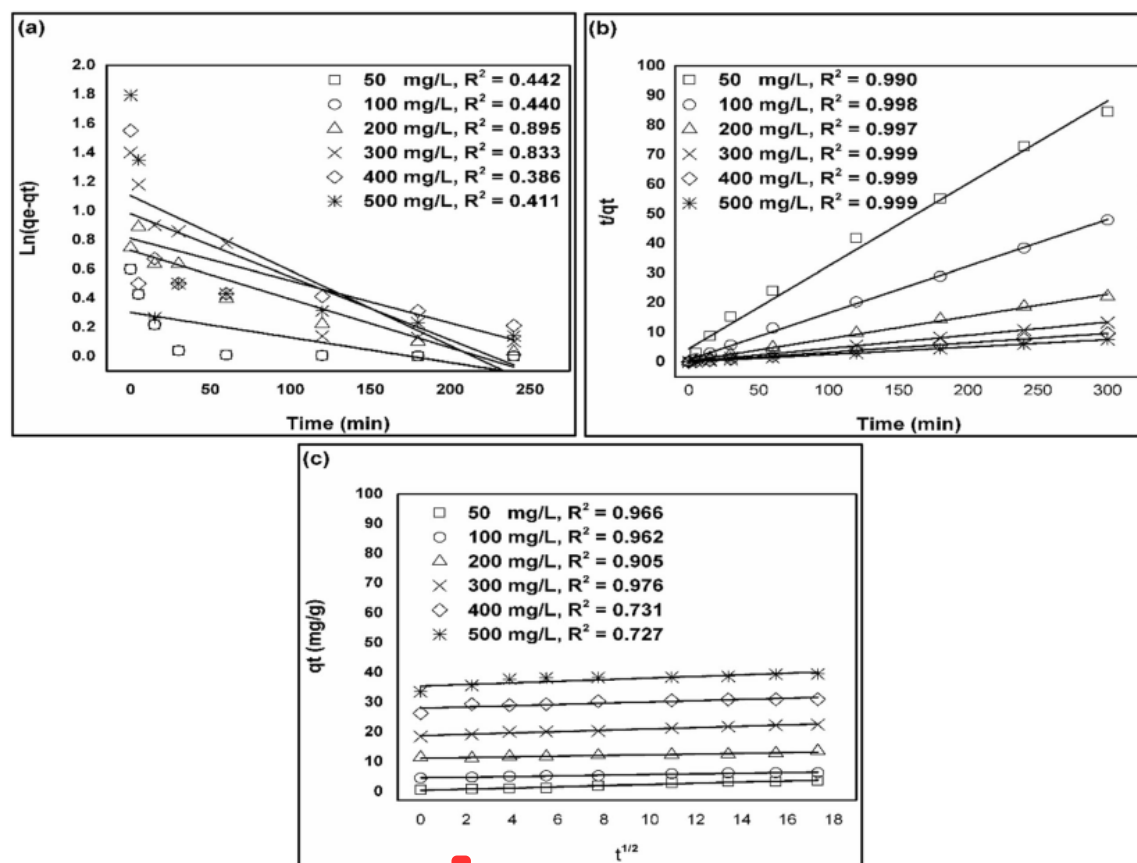
Fig. 2 Kinetics of the SDBS adsorption onto fly ash using **a** pseudo-first-order, **b** pseudo-second-order, and **c** intraparticle models

3.2.2 Effect of SDBS Concentration

The effect of varying the starting concentration of SDBS on the adsorption of SDBS onto fly ash is shown in Fig. 1b. The increase of SDBS concentration from 100 to 2000 mg/L increased the adsorption from 6.259 to 168.821 mg/g and removal efficiency from 62.59 to 84.41% due to a higher amount of SDBS molecules in solution. These molecules occupy the available active bonding sites on fly ash which resulted in a higher adsorption capacity and removal efficiency (Parhizgar et al. 2017). At the highest concentration of SDBS tested (2000 mg/L), the binding did not reach saturation. This indicated that there were still binding sites available on the fly ash adsorbent. The adsorption capacity increases linearly as SDBS concentration is increased from 100 to 2000 mg/L. Removal efficiency increases from 100 to 750 mg/L and then decreases from 750 to 1250 mg/L. Further increasing SDBS concentration above 1250 mg/

L increases removal efficiency. This irregular behavior in the variation of removal efficiency is due to error in the experimental data. The adsorption capacity and removal efficiency are directly related, an increase in one parameter increases the other and vice versa. This type of behavior of increase of adsorption capacity and removal efficiency with increasing surfactant concentration up to 2000 mg/L has rarely been observed in the literature.

3.2.3 Effect of Temperature

The effect of varying the temperature on SDBS removal using fly ash is shown in Fig. 1c. The increase of temperature from 25 to 65 °C decreased the adsorption capacity from 39.752 to 34.435 mg/g and removal efficiency from 79.5 to 68.9%. This could be due to a decrease in the viscosity of the surfactant solution. The decrease of viscosity at higher temperature weakens the

Table 4 Adsorption kinetics of SDBS onto fly ash

Model	SDBS conc (mg/L)	R^2	Q_e, cal. (mg/g)	Q_e, exp. (mg/g)	Model constant	
Pseudo-first-order model	50	0.442	2.009	3.550	0.001	(1/min)
	100	0.440	2.004	6.259	0.001	
	200	0.895	5.345	13.556	0.003	
	300	0.833	12.735	22.475	0.005	
	400	0.386	6.456	31.001	0.002	
	500	0.411	9.549	39.524	0.004	
Pseudo-second-order model	50	0.990	3.584	3.550	0.017	(g/mg min)
	100	0.998	6.369	6.259	0.032	
	200	0.997	13.333	13.556	0.018	
	300	0.999	22.727	22.475	0.014	
	400	0.999	31.25	31.001	0.034	
	500	0.999	39.840	39.524	0.063	
Intraparticle diffusion model	50	0.966	–	–	0.192	mg/g day$^{0.5}$
	100	0.962			0.111	
	200	0.905			0.117	
	300	0.976			0.226	
	400	0.731			0.212	
	500	0.727			0.271	

adsorptive forces between fly ash and SDBS leading to decreased SDBS adsorption. These results show that the adsorption forces between SDBS and fly ash are weak and could indicate that exothermic physisorption is a possible mechanism for SDBS surfactant adsorption onto fly ash adsorbent (Alkan et al. 2005). It shows that the temperature does not support the adsorption of SDBS onto fly ash, rather it supports the desorption of SDBS (Juang et al. 1997). The results indicate that 25 °C is the optimum temperature for adsorbing SDBS onto fly ash as it results in the highest adsorption of surfactant.

3.3 Adsorption Kinetics

The kinetics results obtained by linearly fitting the adsorption data to the pseudo-first-order, pseudo-second-order, and intraparticle diffusion models are shown in Fig. 2a–c. The values of correlation coefficient (R^2), rate constants, and adsorption capacities are given in Table 4.

The correlation coefficient (R^2) of the pseudo-first-order (Fig. 2a) and intraparticle diffusion (Fig.2c) models ranged between 0.38 and 0.89 and between 0.72 and 0.97 respectively. This indicated that these kinetic models did not fit the adsorption data well. The

pseudo-second-order kinetics model had a R^2 of 0.99 (Fig. 2b) for all concentrations tested which indicated that this model fits the adsorption data the best. Furthermore, the predicted adsorption capacities at the initial concentrations of 50, 100, 200, 300, 400, and 500 mg/L obtained using the pseudo-second-order model were similar to the experimentally determined values. From Table 4, the values of rate constant for the pseudo-second-order model ranged between 0.014 and 0.063 indicating a slow adsorption of SDBS onto the fly ash. This was also supported from the equilibrium time of 300 min. The results show that the SDBS removal using fly ash adsorbent follows a pseudo-second-order model and the adsorption is chemisorption. These results are consistent with previous studies which have been reported on SDBS removal using surface-functionalized mesoporous silica nanoparticles and geopolymer (Kim, Kim et al. 2019, Siyal et al. 2019).

3.4 Adsorption Isotherm

Adsorption isotherms of SDBS onto fly ash are shown in Fig. 3a–c. The Langmuir model fits the adsorption data better than the Freundlich and Temkin models and had a correlation coefficient (R^2) of 0.98. The predicted adsorption capacity obtained using this model was
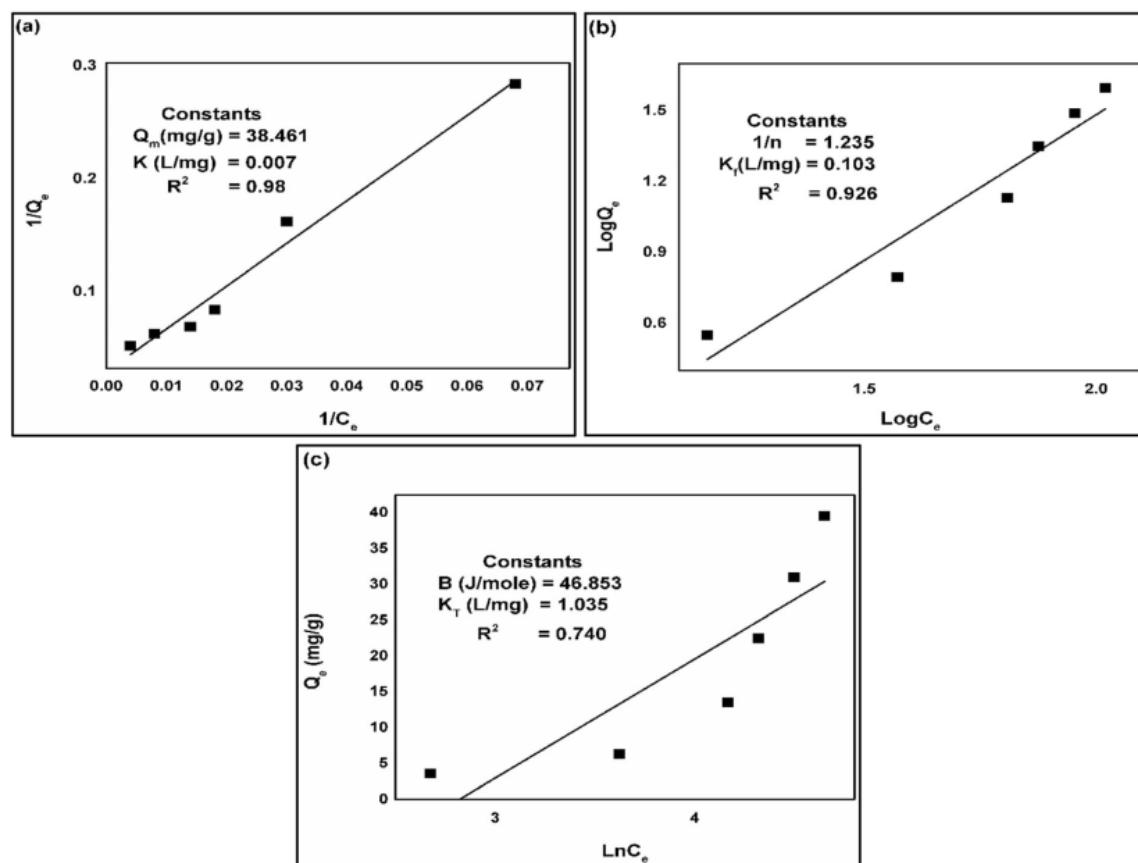
Fig. 3 Adsorption isotherms of SDBS onto fly ash using **a** Langmuir, **b** Freundlich, and **c** Temkin models

38.461 mg/g, which was only 2.7% lower than the experimental adsorption capacity of 39.524 mg/g. The Langmuir rate constant was 0.0015 which indicated the adsorption of SDBS as a slow reaction. It was consistent

Fig. 4 Thermodynamic plot of adsorption of SDBS onto fly ash

with 300 min (5 h) of the required contact time (Siyal et al. 2018).

The Freundlich model had a R^2 value of 0.926, indicating it fits the data better than the Temkin model which had a R^2 of 0.740. The Langmuir isotherm model described the adsorption of SDBS onto fly ash adsorbent as a reaction which is dominated by homogenous distribution of adsorption sites and a monolayer surface coverage, whereas the Freundlich isotherm model suggests that the adsorption occurs due to heterogeneous distribution of adsorption sites with multilayer surface coverage.

However, the Langmuir model fits the experimental data better than the Freundlich model. This indicates that the adsorption of SDBS onto fly ash is a process which occurs due to attraction of the SDBS towards homogenously distributed adsorption sites on the fly ash resulting in the formation of a monolayer of SDBS onto the fly ash. The adsorption isotherm results
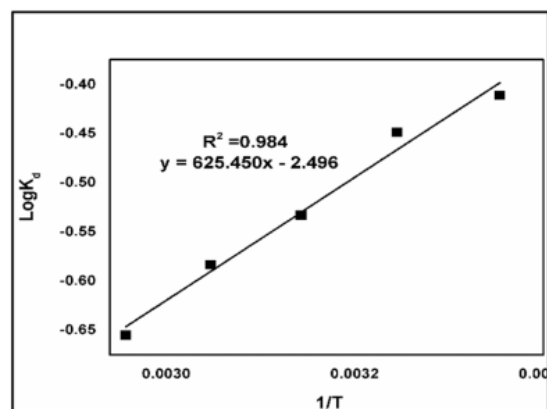
Table 5 Thermodynamic properties of adsorption of SDBS onto fly ash

Thermodynamic property	Value				
E_a (kJ/mol)	− 5.199				
ΔH (kJ/mol)	− 11.975				
ΔS (kJ/mol)	− 47.791				
ΔG (kJ/mol)	14.236	14.714	15.192	15.670	16.148

obtained in this study are consistent with those in other reported studies on the adsorption of SDBS onto amino cross-linked chitosan microspheres (ACCMs) and cross-linked chitosan films (Zhang et al. 2017; Kahya et al. 2018).

3.5 Thermodynamic Properties

The thermodynamic plot and the results of thermodynamic properties are shown in Fig. 4 and Table 5. The adsorption data shows the best fit with R^2 of 0.984. The

Fig. 5 Adsorption mechanism of SDBS onto fly ash

negative activation energy shows that the adsorption of SDBS surfactant onto fly ash does not need activation energy to overcome the barrier. It is a barrierless reaction. The negative enthalpy indicates the adsorption as an exothermic reaction that does not need extra energy for its activation. The enthalpy result ($\Delta H < 0$) indicates that SDBS surfactant is adsorbed through physisorption onto the fly ash adsorbent. Chemisorption is mostly observed at enthalpy above 21 kJ/mol (Liu et al. 2016). The enthalpy results are consistent with the adsorption of SDBS surfactant onto amino cross-linked chitosan microspheres (ACCMs) (Zhang et al. 2017).

The negative entropy value indicates that the disorder of the system at the interface of solid-liquid has reduced. The positive values of Gibbs free energy observed here have rarely been observed in the literature. The positive values of Gibbs free energy indicate the adsorption of SDBS onto fly ash as a non-spontaneous reaction. Non-spontaneous reactions are also called endergonic reactions. Energy is absorbed in such reactions and the total amount of energy required to start such reactions is higher than what is released or generated from the reaction. The Gibbs free energy increased with the increase of temperature from 298.15 to 338.15 K which indicated that the adsorption is more favorable at 298.15 K (Zhang et al. 2017).

3.6 Adsorption Mechanism

The SDBS adsorption onto the fly ash adsorbent followed the pseudo-second-order kinetics model and the Langmuir isotherm model which showed that the adsorption occurred by chemisorption with formation of a monolayer of SDBS onto fly ash. The enthalpy ($\Delta H < 0$) and higher adsorption at a lower temperature of 25 °C indicated the adsorption of SDBS onto fly ash as a physisorption process. Therefore, it could be suggested that SDBS adsorption onto fly ash occurs by both physisorption and chemisorption with monolayer surface coverage.
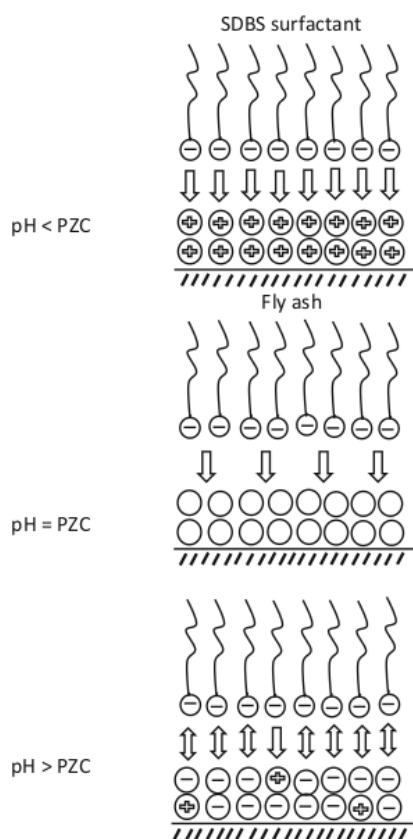
The major portion of adsorption occurs by physisorption, while chemisorption is also involved in the adsorption of SDBS surfactant onto the fly ash adsorbent. This type of mechanism has also been observed in the removal of sulfate onto barium-modified blast-furnace slag geopolymer (Runtti et al. 2016).

The electrostatic charges play a key role in SDBS adsorption onto fly ash. Fly ash is positively charged at pH below 6.58 and negatively charged at pH above 6.58. Fly ash becomes highly positive at pH 2 and the SDBS is negatively charged. The opposite charges increase the affinity of SDBS surfactant towards fly ash which results in SDBS adsorption onto fly ash as shown in Fig. 5. At pH 2, the sulfonate groups (SO_3^-) of the SDBS surfactant react with H^+ ions which results in the SDBS surfactant adsorption onto the fly ash. Other forces such as van der Waal's forces of attraction, hydrogen bonding, and hydrophobic bonding between SDBS and fly ash adsorbent may also play a role in the adsorption.

4 Conclusions

Fly ash can effectively remove the anionic surfactant SDBS from aqueous solution. The optimum conditions for the adsorption of SDBS onto fly ash identified in this study were pH 2 and a temperature of 25 °C. Experimental adsorption data of SDBS onto fly ash fit the pseudo-second-order and Langmuir isotherm models best. The adsorption is an exothermic, barrierless, non-spontaneous, and entropy-reducing reaction which is more promising at a temperature of 25 °C. The enthalpy of -11.975 kJ/mol was obtained. The adsorption of SDBS surfactant onto fly ash occurred by both physisorption and chemisorption with the formation of a monolayer of SDBS on the surface of the fly ash adsorbent. The adsorption occurred by the electrostatic interactions between positively charged fly ash and negatively charged sulfonate group of the SDBS surfactant, while other forces such as hydrogen bonding, hydrophobic bonding, ion exchange, and van der Waal's forces also played a role in the adsorption.

References

Aboulhassan, M., Souabi, S., Yaacoubi, A., & Baudu, M. (2006). Removal of surfactant from industrial wastewaters by coagulation flocculation process. *International Journal of Environmental Science and Technology, 3*(4), 327–332.

Alkan, M., Karadaş, M., Doğan, M., & Demirbaş, Ö. (2005). Adsorption of CTAB onto perlite samples from aqueous solutions. *Journal of Colloid and Interface Science, 291*(2), 309–318.

Asakawa, T., & Ogino, K. (1986). Removal of trace organic compounds from multicomponent liquid mixtures. I. Adsorption of surfactant mixtures on activated carbon. *Colloid and Polymer Science, 264*(12), 1085–1089.

Bautista-Toledo, M. I., Rivera-Utrilla, J., Méndez-Díaz, J. D., Sánchez-Polo, M., & Carrasco-Marín, F. (2014). Removal of the surfactant sodium dodecylbenzenesulfonate from water by processes based on adsorption/bioadsorption and biodegradation. *Journal of Colloid and Interface Science, 418*, 113–119.

Beltrán-Heredia, J., Sánchez-Martín, J., & Barrado-Moreno, M. (2012). Long-chain anionic surfactants in aqueous solution. Removal by Moringa oleifera coagulant. *Chemical Engineering Journal, 180*, 128–136.

Boonyasuwat, S., Chavadej, S., Malakul, P., & Scamehorn, J. F. (2003). Anionic and cationic surfactant recovery from water using a multistage foam fractionator. *Chemical Engineering Journal, 93*(3), 241–252.

De Gisi, S., Lofrano, G., Grassi, M., & Notarnicola, M. (2016). Characteristics and adsorption capacities of low-cost sorbents for wastewater treatment: a review. *Sustainable Materials and Technologies, 9*, 10–40.

Edser, C. (2008). Status of global surfactant markets. *Focus on Surfactants, 2008*(11), 1–2.

Freundlich, H. (1907). Über die adsorption in lösungen. *Zeitschrift für Physikalische Chemie, 57*(1), 385–470.

Gönder, Z., Vergili, I., Kaya, Y., & Barlas, H. (2010). Adsorption of cationic and anionic surfactants onto organic polymer resin Lewatit VPOC 1064 MD PH. *Environmental Geochemistry and Health, 32*(4), 267–273.

Gonzalez-Garcia, C., Gonzalez-Martin, M., Gallardo-Moreno, A., Gomez-Serrano, V., Labajos-Broncano, L., & Bruque, J. (2002). Removal of an ionic surfactant from wastewater by carbon blacks adsorption. *Separation Science and Technology, 37*(12), 2823–2837.

Gupta, S., Pal, A., Ghosh, P. K., & Bandyopadhyay, M. (2003). Performance of waste activated carbon as a low-cost

adsorbent for the removal of anionic surfactant from aquatic environment. *Journal of Environmental Science and Health, Part A, 38*(2), 381–397.

Ho, Y. S., & McKay, G. (1999). Pseudo-second order model for sorption processes. *Process Biochemistry, 34*(5), 451–465.

Ikehata, K., & El-Din, M. G. (2004). Degradation of recalcitrant surfactants in wastewater by ozonation and advanced oxidation processes: a review. *Ozone: Science & Engineering, 26*(4), 327–343.

Juang, R. S., Wu, F. C., & Tseng, R. L. (1997). The ability of activated clay for the adsorption of dyes from aqueous solutions. *Environmental Technology, 18*(5), 525–531.

Kahya, N., Kaygusuz, H., & Erim, F. B. (2018). Aqueous removal of sodium dodecyl benzene sulfonate (SDBS) by crosslinked chitosan films. *Journal of Polymers and the Environment, 26*(5), 2166–2172.

Kim, D., Kim, J., Lee, K.-W., & Lee, T. S. (2019). Removal of sodium dodecylbenzenesulfonate using surface-functionalized mesoporous silica nanoparticles. *Microporous and Mesoporous Materials, 275*, 270–277.

Kimerle, R. A., & Swisher, R. (1977). Reduction of aquatic toxicity of linear alkylbenzene sulfonate (LAS) by biodegradation. *Water Research, 11*(1), 31–37.

Kowalska, I. (2011). Ion-exchange–ultrafiltration system for surfactants removal from water solutions. *Desalination and Water Treatment, 25*(1–3), 47–53.

Krawczyk, J. (2018). Thermodynamic properties of disaccharide based surfactants adsorption at the water-air interface. *Colloids and Surfaces A: Physicochemical and Engineering Aspects, 551*, 50–57.

Lagergren, S. (1898). About the theory of so-called adsorption of soluble substances. *Sven Vetenskapsakad Handingarl, 24*, 1–39.

Langmuir, I. (1918). The adsorption of gases on plane surfaces of glass, mica and platinum. *Journal of the American Chemical Society, 40*(9), 1361–1403.

Liu, Y., Yan, C., Zhang, Z., Wang, H., Zhou, S., & Zhou, W. (2016). A comparative study on fly ash, geopolymer and faujasite block for Pb removal from aqueous solution. *Fuel, 185*, 181–189.

Ncibi, M. C., Gaspard, S., & Sillanpää, M. (2015). As-synthesized multi-walled carbon nanotubes for the removal of ionic and non-ionic surfactants. *Journal of Hazardous Materials, 286*, 195–203.

Önder, E., Koparal, A. S., & Öğütveren, Ü. B. (2007). An alternative method for the removal of surfactants from water: electrochemical coagulation. *Separation and Purification Technology, 52*(3), 527–532.

Pal, A., Pan, S., & Saha, S. (2013). Synergistically improved adsorption of anionic surfactant and crystal violet on chitosan hydrogel beads. *Chemical Engineering Journal, 217*, 426–434.

Panizza, M., Delucchi, M., & Cerisola, G. (2005). Electrochemical degradation of anionic surfactants. *Journal of Applied Electrochemistry, 35*(4), 357–361.

Parhizgar, F., Alishahi, A., Varasteh, H., & Rezaee, H. (2017). Removing sodium dodecyl benzene sulfonate (SDBS) from aqueous solutions using chitosan. *Journal of Polymers and the Environment, 25*(3), 836–843.

Pereira, L. C., de Souza, A. O., Bernardes, M. F. F., Pazin, M., Tasso, M. J., Pereira, P. H., & Dorta, D. J. (2015). A perspective on the potential risks of emerging contaminants to human and environmental health. *Environmental Science and Pollution Research, 22*(18), 13800–13823.

Pérez-Carrera, E., León, V. M., Lara-Martín, P. A., & González-Mazo, E. (2010). Influence of the hydrophilic moiety of anionic and nonionic surfactants on their aerobic biodegradation in seawater. *Science of the Total Environment, 408*(4), 922–930.

Runtti, H., Luukkonen, T., Niskanen, M., Tuomikoski, S., Kangas, T., Tynjälä, P., Tolonen, E.-T., Sarkkinen, M., Kemppainen, K., Rämö, J., & Lassi, U. (2016). Sulphate removal over barium-modified blast-furnace-slag geopolymer. *Journal of Hazardous Materials, 317*, 373–384.

Schouten, N., van der Ham, L. G., Euverink, G.-J. W., & de Haan, A. B. (2007). Selection and evaluation of adsorbents for the removal of anionic surfactants from laundry rinsing water. *Water Research, 41*(18), 4233–4241.

Shamsuddin, R. M., Verbeek, C. J. R., & Lay, M. C. (2014). Producing protein intercalated bentonite — equilibrium, kinetics and physical properties of gelatin–bentonite system. *Applied Clay Science, 87*, 52–60.

Sineva, A. V., Parfenova, A. M., & Fedorova, A. A. (2007). Adsorption of micelle forming and non-micelle forming surfactants on the adsorbents of different nature. *Colloids and Surfaces A: Physicochemical and Engineering Aspects, 306*(1), 68–74.

Siyal, A. A., K. A. Azizli, L. Ismail, Z. Man and M. I. Khan (2016). Suitability of Malaysian fly ash for geopolymer synthesis. Advanced Materials Research, Trans Tech Publ.

Siyal, A. A., Rashid Shamsuddin, M., Rabat, N. E., Zulfiqar, M., Ayoub, M., & Azizli, K. A. (2018). Removal of anionic surfactant sodium dodecylbenzenesulfonate from water using fly ash adsorbent. *IOP Conference Series: Materials Science and Engineering, 458*, 012043.

Siyal, A. A., Shamsuddin, M. R., Rabat, N. E., Zulfiqar, M., Man, Z., & Low, A. (2019). Fly ash based geopolymer for the adsorption of anionic surfactant from aqueous solution. *Journal of Cleaner Production, 229*, 232–243.

Siyal, A. A., Shamsuddin, M. R., Low, A., & Rabat, N. E. (2020). A review on recent developments in the adsorption of surfactants from wastewater. *Journal of Environmental Management, 254*, 109797.

Taffarel, S. R., & Rubio, J. (2010). Adsorption of sodium dodecyl benzene sulfonate from aqueous solution using a modified natural zeolite with CTAB. *Minerals Engineering, 23*(10), 771–779.

Temkin, M. I. (1941). Adsorption equilibrium and the kinetics of processes on nonhomogeneous surfaces and in the interaction between adsorbed molecules. *Zh Fiz Chim, 15*, 296–332.

Tezel, U., Tandukar, M., Martinez, R. J., Sobecky, P. A., & Pavlostathis, S. G. (2012). Aerobic biotransformation of n-tetradecylbenzyldimethylammonium chloride by an enriched pseudomonas spp. community. *Environmental Science & Technology, 46*(16), 8714–8722.

Valizadeh, S., Younesi, H., & Bahramifar, N. (2016). Highly mesoporous K_2CO_3 and KOH/activated carbon for SDBS removal from water samples: batch and fixed-bed column adsorption process. *Environmental Nanotechnology, Monitoring & Management, 6*, 1–13.

Visa, M., & Duta, A. (2013). TiO$_2$/fly ash novel substrate for simultaneous removal of heavy metals and surfactants. *Chemical Engineering Journal, 223*, 860–868.

Wang, S., Boyjoo, Y., Choueib, A., & Zhu, Z. H. (2005). Removal of dyes from aqueous solution using fly ash and red mud. *Water Research, 39*(1), 129–138.

Wang, S., Terdkiatburana, T., & Tadé, M. O. (2008). Single and co-adsorption of heavy metals and humic acid on fly ash. *Separation and Purification Technology, 58*(3), 353–358.

Weber, W. J., & Morris, J. C. (1963). Kinetics of adsorption on carbon from solution. *Journal of the Sanitary Engineering Division, 89*(2), 31–60.

Zanoletti, A., Federici, S., Borgese, L., Bergese, P., Ferroni, M., Depero, L. E., & Bontempi, E. (2017). Embodied energy as key parameter for sustainable materials selection: the case of reusing coal fly ash for removing anionic surfactants. *Journal of Cleaner Production, 141*, 230–236.

Zhang, C., Valsaraj, K. T., Constant, W. D., & Roy, D. (1999). Aerobic biodegradation kinetics of four anionic and nonionic surfactants at sub-and supra-critical micelle concentrations (CMCs). *Water Research, 33*(1), 115–124.

Zhang, C., Wen, H., Huang, Y., & Shi, W. (2017). Adsorption of anionic surfactants from aqueous solution by high content of primary amino crosslinked chitosan microspheres. *International Journal of Biological Macromolecules, 97*, 635–641.

Zulfiqar, M., Chowdhury, S., Samsudin, M. F. R., Siyal, A. A., Omar, A. A., Ahmad, T., & Sufian, S. (2020). Effect of organic solvents on the growth of TiO$_2$ nanotubes: an insight into photocatalytic degradation and adsorption studies. *Journal of Water Process Engineering, 37*, 101491.

Springer

Adsorption Kinetics, Isotherms, and Thermodynamics of Removal of Anionic Surfactant from Aqueous Solution Using Fly Ash